Does Water Activity Rule *P. mirabilis* Periodic Swarming? I. Biochemical and Functional Properties of the Extracellular Matrix

Elodie Lahaye,[†] Thierry Aubry,[‡] Nelly Kervarec,[§] Philippe Douzenel,[†] and Olivier Sire*[,†]

Laboratoire des Polymères, Propriétés aux Interfaces et Composites, Université de Bretagne-Sud, Campus de Tohannic, BP573 56017 Vannes Cedex, France, Laboratoire de Rhéologie, Université de Bretagne Occidentale, 6 Avenue Le Gorgeu CS93837, 29238 Brest Cedex 3, France, and Service Commun de Recherche de Résonance Magnétique Nucléaire et Résonance Paramagnétique Electronique de l'Université de Bretagne Occidentale, 6 Avenue Le Gorgeu CS93837, 29238 Brest Cedex 3, France

Received December 13, 2006; Revised Manuscript Received January 19, 2007

The dynamics of bacterial colonies is complex in nature because it correlates the behavior of numerous individual cells in space and time and is characterized by emergent properties such as virulence or antibiotics resistance. Because there is no clear-cut evidence that periodic swarming of *P. mirabilis* colonies is ruled by chemical triggers responsible for cell-to-cell signaling in most of the biofilms, we propose that the observed periodicity relies on the colony's global properties. Hence, the biochemical and functional properties of the extracellular matrix (ECM) of *P. mirabilis* colonies were investigated. A binary exopolysaccharide mixture (1 and 300 kDa), glycinebetaine, and a phenoglycolipid were identified. Rheology, calorimetry, and water sorption experiments performed on purified EPS bring evidence that these exoproducts exhibit marked viscoelasticity, which likely relies on large scale H bond networks. Such behavior is discussed in terms of water activity because the mechanical ECM properties were found to depend on hydration.

Introduction

Bacterial biofilms are the most current forms of bacterial life.[1] For better or for worse, such multicellular entities are subject to complex regulations that mainly rely on sophisticated cell-to-cell communications such as quorum sensing.[2] Such mechanisms allow each bacterial cell to "sense" the local population density, which in turn will result in emergent properties, such as virulence, resistance to antibiotics, and massive exoproducts synthesis. Though the role of chemical triggers such as homoserine lactone (AHL) or furanone has been well assessed in model biofilms,[3−4] some exceptions exist. In particular, the *Proteus mirabilis* colonies present some provocative features because they are characterized by the alternation of two phenotypes, swarming and vegetative,[5−6] which allows the population to actively colonize a Petri dish within a few hours through periodic swarming and consolidation phases.[7−8] This results in a typical bull's eye pattern with concentric rings. *P. mirabilis* can hitherto be considered as a biological oscillator, whose dynamics is characterized by a robust periodicity and synchrony that links billions of individual cells. Despite this remarkable behavior, there is no clear-cut evidence for the existence of extracellular signal molecules except in the very early phases of initial differentiation when a liquid culture inoculum is deposited on an agar support.[9] It has been proposed that the *rsbA* gene has both positive and negative functions in regulating swarming migration;[10] however, the authors only observe a decreased initial lag period but no differences in further periodic behavior between wild type and defective bacteria. Besides, different metabolites, such as putrescine[11] or glutamine,[12] have been identified as essential for swarming migration, but no obvious regulatory function has been evidenced. In previous studies,[13−14] we have characterized the time sequence of the differentiation process from vegetative to swarm phenotypes and also mapped the space and time distributions of the two populations. The colony's multicellular entity undergoes mass migration through alternative swarming and consolidation. Swarming only concerns the distal part of the colony because this phenotype is restricted to the active colony's edge. In more inner domains, live vegetative cells predominate. From the dynamic point of view, the colony has to face two apparently opposite goals, which are spatial expansion and entity cohesion. This is solved by the cessation of periodic motion, which triggers every consolidation phase. One still wonders about the nature of the signal that repeatedly stops the expansion because no conventional trigger is produced, and the cells are not fuel-exhausted.[15] This led us to consider more precisely the multicellular entity as a whole. A *P. mirabilis* colony is made of a large number of individual cells that live, swarm, and differentiate into a continuum that they have synthesized on their own. This extracellular matrix (ECM) is necessarily involved in the periodicity and synchrony macroscopically observed. Strangely, to our knowledge, no study has been aimed at characterizing the *P. mirabilis* ECM. We, therefore, propose a global approach of this continuum to determine both its biochemical composition and functional properties. The idea that the order present in a dynamic system would depend on global, emergent properties is not new, but it has not been applied to bacterial colonies. Understanding a colony's dynamics undoubtedly requires a pluridisciplinary approach. Molecular biology has allowed the identification of the *flhDC* operon, which rules the differentiation process,[16] but has not permitted

* Corresponding author. E-mail: osire@univ-ubs.fr. Phone: ++ 33 297 017 148. Fax: ++ 33 297 017 071.

[†] Université de Bretagne-Sud.

[‡] Laboratoire de Rhéologie, Université de Bretagne Occidentale.

[§] Recherche de Résonance Magnétique Nucléaire et Résonance Paramagnétique Electronique de l'Université de Bretagne Occidentale.

10.1021/bm061181l CCC: $37.00
Published on Web 03/14/2007

the understanding of how and why it is switched on and off. *In situ* biophysics has allowed us to map in space and time the swarm and vegetative populations[13−14] but has not allowed us to understand why swarmers stop migration periodically and synchronously. The present article and the next aim at demonstrating that global mechanical properties of the ECM play a major role in the colony's dynamic pacing.

Experimental Section

Strain, Media, and Culture Conditions. The *P. mirabilis* wild type strain WT19 corresponds to the clinical isolate U6450.[5] WT19 was grown in LB medium at 37 °C. To obtain homogeneous populations of swarmer bacteria, 200 μL of an overnight liquid culture was spread onto a LB agar (1.5%) plate, and the latter was incubated for 4 h at 37 °C. For the examination of the level of bacterial elongation and population homogeneity, the cells were resuspended in LB with 1% formaldehyde, and 4,6-diamino-2-phenylindole (DAPI) was added (final concentration of 0.25 μg/mL). DAPI is a fluorescent dye that allows the visualization of bacterial chromosomes,[17] which was achieved by examination under an epifluorescence microscope (Olympus BX-60) with UV excitation and visible emission (380 nm cutoff). The elongation level was assessed by counting the number of nucleoids per cell (21 ± 4) as well as by measuring the bacterial rod lengths (41 ± 14 μm). Cells liquid cultures were similarly performed at 37 °C in LB medium without agar.

Experimental Techniques. *ECM Biochemical Characterization.* After 4 h, *P. mirabilis* colonies are gently scratched off the agar, the corresponding volume and mass are measured, and the sample is diluted 2-times with an isotonic NaCl solution (4 °C). Bacterial cells are pelleted at 8000*g* (20 min, 4 °C), and the supernatant containing the ECM constituents is stored at 4 °C in the presence of a few micrograms of sodium azide to prevent any further bacterial contamination. The volume of the cell pellet is measured to determine the cell/ECM volume ratio.

Protein Assay. Proteins of the ECM are conventionally assayed according the Bradford method,[18] and molecular mass distribution is analyzed by SDS−PAGE.[19]

Exopolysaccharides Extraction and Purification. A 1.5 volume of ice-cold absolute ethanol is added to the ECM sample, and the solution is stored overnight at −20 °C. The precipitated EPS are then collected by centrifugation (2000*g* for 10 min), recovered, and dried at 37 °C. The molecular weight distributions of the EPS are analyzed by size exclusion chromatography. Then, 10 mg of dried EPS are dissolved in 1 mL of distilled water and analyzed by SEC. The XK26 column used (25 mm × 620 mm, Pharmacia Biotech, France**)** is furnished with a Sephacryl S-300 HR (Sigma-Aldrich, France) resin. The sample (1 mL) is injected and eluted at ambient temperature using 0.3 mL/min 0.5 M NaCl. Detection is performed using an Iota 2 (Dionex, France) refractive index detector. Fractions of 5 mL are collected using a Gilson fraction collector. The different EPS fractions are pooled and dried under vacuum. The EPS sugar composition is determined using acid hydrolysis. The EPS is treated with 2 M HCl for 24 h at 100 °C. The released sugars are analyzed using high performance anion exchange chromatography (HPAEC) with pulsed amperometric detection (PAD) using a Dionex system. Samples are injected in a Carbopac PA-1 column (4 × 250 mm) with a Carbopac PA-1 guard column (4 × 50 mm), and separation is performed at 1 mL/min by isocratic elution with 20 mM NaOH for 30 min, followed by a linear gradient from 20 to 100 mM NaOH with 1 M sodium acetate in 10 min. This gradient is maintained for 10 min and then returned to 200 mM NaOH.

Lipid Extraction and Purification. Lipid extraction is carried out by the method of Bligh and Dyer.[20] Colonies are diluted in an isotonic NaCl solution as described above, cells are pelleted, and the supernatant containing the ECM exoproducts is acidified to pH 2 prior to the addition of 3 volumes of a chloroform/methanol mixture (2/1). After 2 min of agitation, the phases are allowed to separate, and the organic phase is evaporated to dryness at 30 °C by using a Rotavapor. Lipid characterization is then achieved by thin-layer chromatography: 20 mg of the dry lipid extract is dissolved in 100 μL of CH_3Cl/MeOH (2/1) and deposited on an activated 20 × 20 cm K6 silicagel plate (Whatmann, Inc.), and separation is performed in a tank saturated with a CH_3Cl/MeOH/H_2O (80/18/2) mixture. Neutral glycolipids are revealed by anthrone.[21]

NMR Spectroscopy. One- and two-dimensional NMR spectra were recorded at 25 °C on a Bruker Avance 500 spectrometer equipped with an indirect 5 mm triple resonance probe head TXI $^1H/^{31}P/^{13}C$. NMR analyses were performed on the whole ECM fraction by dissolution in 700 μL of a 100% D_2O solution. Neutral glycolipid samples were analyzed by dissolution in 700 μL of $CDCl_3$/MeOD (2/1). Chemical shifts were expressed in ppm relative to TMS as the external reference. Double-quantum filtered ^1H-^1H correlated spectroscopy (DQF COSY), heteronuclear multiple quantum coherence ^1H-^{13}C (HMQC), and heteronuclear multiple bond coherence ^1H-^{13}C (HMBC) with a delay of 60 ms were performed according to standard pulse sequences to assign ^1H and ^{13}C resonances. For example, in an HMQC experiment, the raw data set consisted of 128 fid of 1024 (F2) * 128 (F1) complex data points, each zero-filled to 1 k in the F1 dimension prior to Fourier transform spectroscopy with a spectral width of 25162 and 3822 Hz in the F1 and F2 dimensions, respectively, with a 30° pulse, a delay of 2 s, and 128 scans.

Fluorescence. Experiments are realized by using an SLM 8100 fluorimeter. Dry lipid extracts were solubilized in 1 mL of chloroform, and both emission (305 nm excitation) and excitation (emission at 340 nm) spectra were collected at 20 °C.

EPS Rheology. The viscous properties of EPS solutions at concentrations ranging from 40 to 100 g/L have been measured using a Contraves Low-Shear 30 viscometer, equipped with a Couette device. For these low concentration solutions, it was impossible to determine any viscoelastic properties. However, for EPS solutions at concentrations ranging from 100 to 300 g/L, viscoelastic properties have been characterized by performing oscillatory simple shear experiments with a controlled stress and a controlled strain rotational rheometer. The controlled strain Rheometrics ARES rheometer was equipped with a cone and plate geometry (cone angle, 3°59′; diameter, 4 cm), and the controlled stress Carri-Med CSL 50 rheometer was equipped with a parallel plate geometry (diameter, 4 cm; gap, 500 μm). All rheometric measurements were performed at 37 °C. A thin layer of low-viscosity silicone oil was placed on the air/sample interface in order to minimize water evaporation. For all samples tested, the extent of the linear viscoelastic regime was determined at 1 Hz, prior to any frequency sweep measurements. The linear viscoelastic regime is characterized by a sinusoidal response and the proportionality of the response to excitation. The linear viscoelastic properties were studied over a 2 decade frequency range: from 10^{-2} Hz to 1 Hz. The frequency range used in this spectro-mechanical investigation is limited because of the relatively high temperature imposed during the tests.

ATR-FTIR Spectroscopy. FTIR experiments were performed in the attenuated total reflection (ATR) mode using a Protégé 460 spectrometer and a thermostated (37 °C) horizontal *ZnSe* crystal ($n = 2.4$). The spectrometer is fitted with a DTGS detector. Each spectrum is acquired at a 4 cm^{-1} resolution and represents the accumulation of 128 separate scans. A hydrated EPS solution (100 μL) is deposited on the crystal and allowed to slowly dehydrate. Four cycles of water sorption/desorption are performed while FTIR spectra are continuously recorded with a time step of about 2 min. Water sorption is favored by saturating the atmosphere above the solution in water. This yields a 51 spectra matrix, which corresponds to various hydration levels. For a particular spectrum, hydration is estimated after the optical density at 750 cm^{-1} corresponds to the upper tail of the water δ_L libration band[22−23] located at 620 cm^{-1}. Considering the initial anhydrous spectrum with a 0% relative humidity (RH), and the final, fully hydrated spectrum with a 100% RH, the %RH of each spectrum is calculated from the $OD_{750\ cm^{-1}}$ according to the following equation.

$$RH(\%) = 100 \times \frac{OD - OD_{INIT}}{OD_{FINAL} - OD_{INIT}}$$

Spectral data are further treated by using The Unscrambler software (Camo, Norway) for spectral normalization and principal components analysis (PCA).

Polarizing Microscopy. EPS solutions are allowed to age between a sealed slide and coverslip. Observations are performed by using a BX-60 polarizing microscope and a quarter waveplate.

Differential Scanning Calorimetry. EPS solutions are subjected to calorimetry analysis by using a DSC822^e calorimeter (Mettler, Toledo). Initially, 40 μL of a 100 g/L solution is placed in a pierced aluminum pan. Temperature ramps are sequentially performed between −100 and 80 °C at a 20 °C min^{-1} rate. Starting at 25 °C, the sample is progressively heated to 80 °C, stabilization is allowed for 2 min, cooling is performed down to −100 °C, stabilization is again performed for 2 min, and the sample is heated to 80 °C and then allowed to cool down to 25 °C. At this moment, the sample is weighed to measure the loss of water and to calculate the new sample concentration. Then a new cycle is initiated. This protocol allows us to vary the EPS concentration from 100 to 550 g/L.

Results and Discussion

Colony's Biometry. *P. mirabilis* colonizes a Petri dish in a few hours through periodic swarming and consolidation phases.[8] Video recordings and confocal microscopy imaging have allowed the measurement of colony dimensionalities.[14] Under the experimental conditions used in our laboratory, a swarming phase lasts about 1 h, during which the colony radius is increased by 2 mm. Local video recordings show that the colony edge progresses at a 1 μm/s rate with bacterial raft internal bioconvection motions as fast as 30 μm/s. Besides, as revealed by Live/Dead dyeing, the colony exhibits a 16 μm thickness, whereas the remnants of consolidation phases, the terraces, present a local thickening of 45 μm. As shown previously,[14] the swarmer population is strictly limited in the most recent external migration phase. Mass and volume measurements have been performed to quantify the relative proportions of cells and ECM in which the population lives. The ECM represents 20% in mass of the whole colony. A relatively low hydration level has been determined by gravimetry because a ratio of 3.5 g of water per g of colony (d.w.) has been measured.

EPS Molecular Size Distribution. Exopolysaccharides are the most common exoproducts in bacterial slimes. Attempts have thus been performed to analyze the EPS present in the *P. mirabilis* slime. To our knowledge, no study was focused on the exoproducts of this bacterium because literature only reports on capsular polysaccharides (CPS).[24−26] EPS were quantified in the ECM fraction and revealed that they feature about 30% in mass of the ECM. Cold ethanolic precipitates from ECM were analyzed by size exclusion chromatography (Figure 1). This reveals that two components are present: a preponderant low MW component of 1 kDa (retention time of 149 min), which features 98% of the EPS produced, and a minor high MW component of 300 kDa (retention time of 339 min). To check whether this unusual binary composition was somehow dependent on the bacterial environment, EPS size distribution was also studied in a colony that was grown on 2.5% agar (as compared to standard conditions of 1.5%) and in a liquid culture. In the first condition (2.5% agar), the amount of the 1 kDa component is slightly decreased (91%) to the benefit of a new component exhibiting a MW of 13 kDa (retention time of 255 min). In a liquid culture, this size distribution is markedly altered because the low (1 kDa) and high (300 kDa) components are

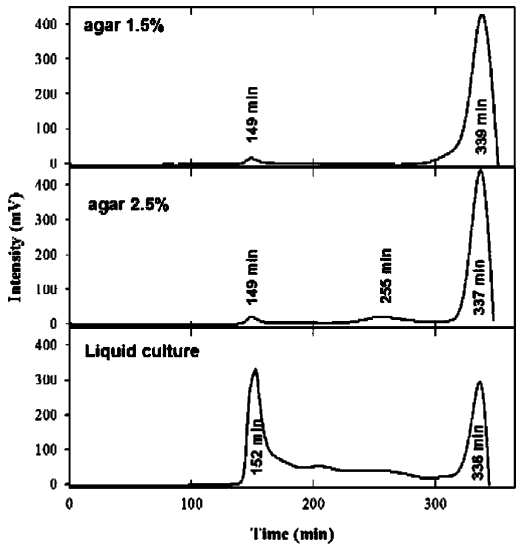

Figure 1. EPS size exclusion chromatography. The EPS size distribution has been analyzed in colonies at two agar concentrations (upper panels) and in liquid culture conditions (lower panel).

synthesized in equal amounts. From this, it appears that depending on the bacterial growth conditions, the EPS production qualitatively varies. Besides, the major component produced within the colony exhibits an unusually low MW because most of the EPS observed in colonies present much higher sizes ranging from 50 to 500 kDa.[27] A polysaccharide of 1 kDa corresponds to a 5 unit polymer. Because this is close to the saccharide moiety of membrane lipopolysaccharides (LPS), it was assessed, through the detection of KDO, a sugar specific to LPS, that the presence of this component was not due to LPS contamination (data not shown). The physiological significance of such a small component within the colony will be discussed later.

EPS Sugar Composition. The sugar composition of the 1 and 300 kDa EPS compounds produced on a 1.5% agar substratum by *P. mirabilis* was analyzed through HPAEC. Figure 2 shows the corresponding profiles along with the standards used. Clearly, the sugar composition of the two compounds varies, which rules out the possibility that the 1 kDa compound may be derived from the hydrolysis of the large component. The 1 kDa component is mainly composed of rhamnose and glucose (peaks 1 and 5, respectively), whereas rhamnose, galactosamine, glucose, and mannose (peaks 1, 2, 5, and 6, respectively) are present in the 300 kDa component. *P. mirabilis* CPS[24−26] is acidic because of the presence of at least one uronic acid unit. This negatively charged sugar was looked for in the purified EPS fraction without success. This further supports that the low MW EPS component does not derive from membrane capsular polysaccharides. It must also be noted that an unidentified sugar is present in both EPS compounds (peak X in Figure 2).

Lipid Analysis. The ECM biochemical study revealed that lipids were significantly present in the *P. mirabilis* slime because they feature 15% of the ECM in mass. This unusually high level drove us to further characterize the biochemical nature of these lipids. Because rhamnolipids, though never reported in *P. mirabilis* colonies, are commonly observed in model *Pseudomonas* biofilms,[28] we first made attempts to detect this glycolipid in the *P. mirabilis* colony. Accordingly, we performed the semiquantitative test for extracellular rhamnolipid detection, initially set up by Siegmund and Wagner.[29] Except for the fact that $CaCl_2$ (0.2 g/L) was preferred in place of cetyl-trimethy-

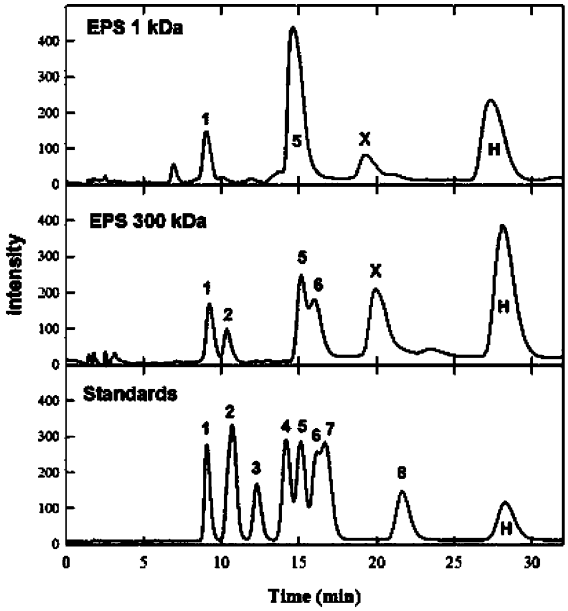

Figure 2. EPS sugar composition analyzed by HPLC. The Figure displays the sugar composition of the two compounds purified by SEC chromatography. The lower panel displays the elution pattern of the standards 1, rhamnose; 2, galactosamine; 3, glucosamine; and 4, galactose, and 5, glucose; H, heptose used as a standard; and X, unknown.

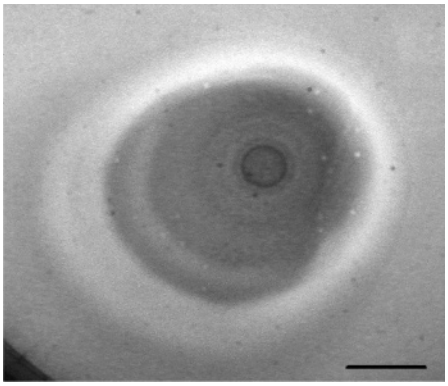

Figure 3. Blue methylene dye for glycoplipid detection in biofilm. The bar = 1 cm.

lammonium bromide, which inhibits bacterial expansion, the test was conducted as described by these authors. Figure 3 clearly shows alternating dark (blue) and light concentric rings around the inoculum. This arises from the formation of an insoluble complex between the anionic biosurfactant and the basic dye methylene blue. The localization of the dark rings strongly suggests that the biosurfactant is synthesized before active swarming, during the consolidation phase, which matches well the findings of a previous study.[13]

The lipid ECM extract was then analyzed by TLC. Among different spots, a component exhibiting a 0.66 front ratio was observed to react with anthrone, a dye specific for neutral sugar[21] (data not shown). Anthrone is currently used for rhamnolipid detection. Such a front ratio is closed to that observed for mono-rhamnolipids in such a solvent system ($CH_3Cl/MeOH/H_2O$, 80/18/2).[30] Additionally, the fatty acid composition of the lipid extract was analyzed by gas chromatography and revealed that besides long chain (C16 to C20) fatty acid compounds, a C12 lauric acid component was identified. This matches well the chain lengths observed in bacterial biosurfactants.[31]

Further analyses were performed by NMR spectroscopy. Aliphatics were characterized by signals at 1−1.3 ppm in the

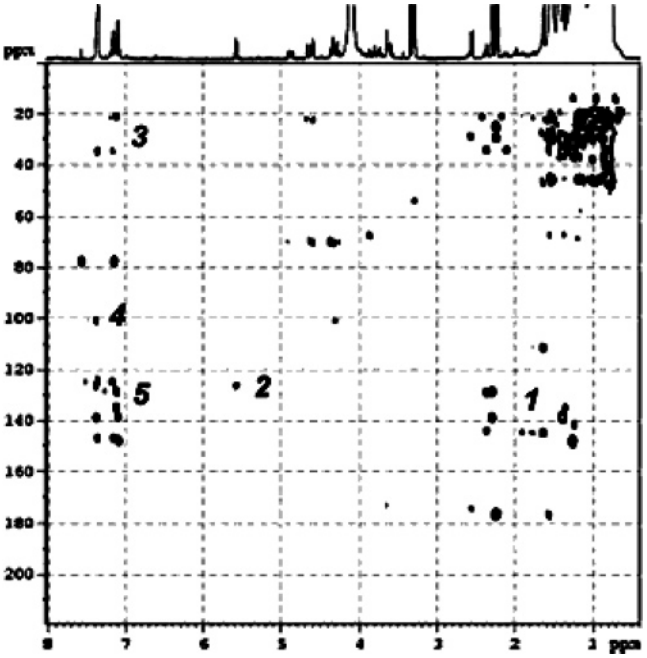

Figure 4. ^1H-^{13}C (HMBC) at 25 °C in $CDCl_3$/MeOD (2/1). Cross-peak numbering is as follows: 1, between aliphatics and aromatics; 2, between H1 sugar and aromatics; 3, between aromatics and aliphatics; 4, between aromatics and C1 of sugar; and 5, between aromatics.

^1H NMR spectrum. From the HMBC spectrum (Figure 4), it can be inferred that those signals are bound to aromatics ring carbons showing up at 130 ppm. The ^1H signal at 5.5 ppm is also characteristic of the H1 of a sugar and correlated with carbon at 125 ppm, assigned to aromatics rings. The ^1H signals of aromatics at 7.2−7.5 ppm clearly show correlations with aliphatic carbons at 21 and 35 ppm, C1 of the sugar at 101 ppm, and other aromatic carbons at 125−150 ppm. These assignments not only confirm that glycolipids are actually produced by *P. mirabilis* but also indicate that an aromatic group is present. This aromatic moiety lacking in *Pseudomonas* rhamnolipids, the glycolipids synthesized by *P. mirabilis*, must be distinct in nature. The concomitant presence of a sugar, a lipid, and an aromatic ring suggests that a phenoglycolipid (PGL) could be produced. Such PGLs have only been identified in the *Mycobacterium* genus, which is the bacterium genus responsible for leprosy and tuberculosis.[32−34] The structure of PGL has been studied in various *Mycobacterium* strains through NMR and IR spectroscopies.[34] The glycosyl substitute is a mono-, di-, or tri-rhamnopyranose and/or glucopyranose.

To confirm the biochemical nature of this compound, spectroscopic experiments have been performed (Figure 5). The UV absorption spectrum collected in $CHCl_3$ and its second derivative exhibit two electronic transitions located at 273 and 284 nm, which correspond to $\pi \rightarrow \pi^*$ transitions characteristic of aromatic compounds. Fluorescence excitation and emission spectra show a maximal exc/emi couple at 305 nm/340 nm, which is observed for substituted phenolic groups. Finally, the glycolipid infrared spectrum was collected in the ATR mode. The corresponding spectrum shows main absorption bands at 2916, 1712 , 1212, and 1160 cm^{-1}, which correspond to methylene and methyl groups, carbonyl ester bonds, and sugar rings, respectively. This spectrum is very similar to those previously reported for various *Mycobacterium* species.[35−37] As a whole, even though the glycosyl substituent has not been characterized, these findings strongly suggest that *P. mirabilis* synthesizes a PGL during the colonization process.

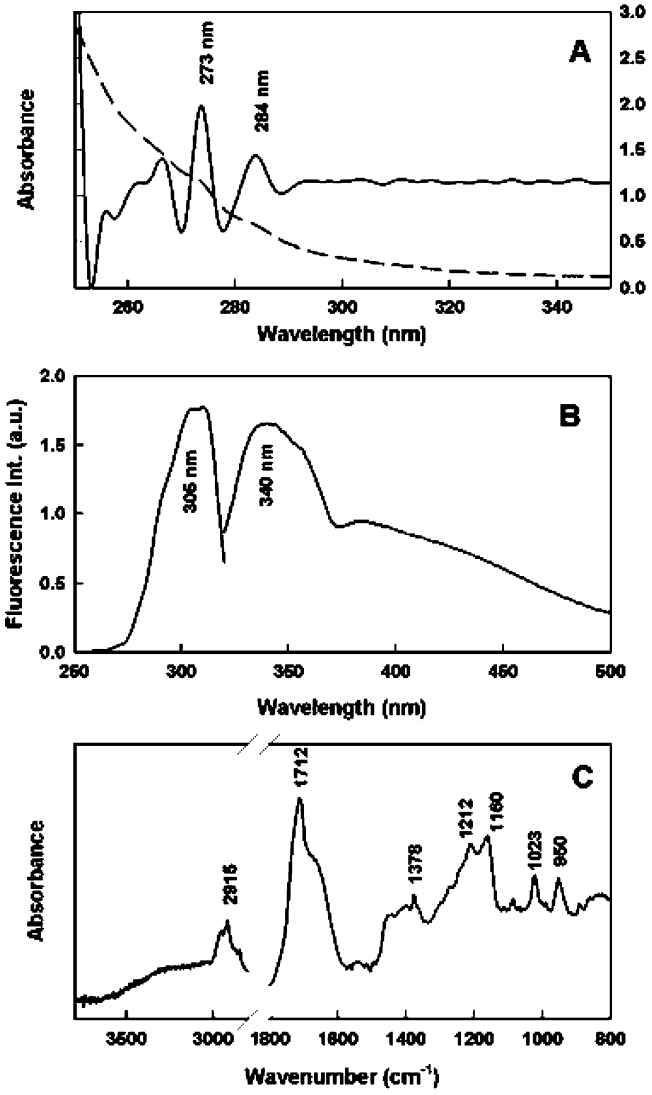

Figure 5. Fluorescence emission and UV and IR absorbance spectra of the ECM lipid extract. (A) UV absorption spectrum and its inverted second derivative. (B) Fluorescence excitation and emission spectra. (C) Mid infrared spectrum.

Glycinebetaine. ^{1}H NMR experiments performed in pure D_2O have revealed two peaks characteristic of glycinebetaine (GB), $(CH_3)_3$-$^+$N-CH_2-COO^-, which is an osmoprotectant synthesized or accumulated by bacteria experiencing an osmotic shock. This compound is considered a compatible solute because bacteria accumulate GB in proportion to the osmotic stress up to molar concentrations without any metabolite interferences.[38] Figure 6, displaying a partial ECM ^{1}H NMR spectrum, shows two peaks at 3.88 and 3.24 ppm corresponding to the methylene and the three methyl of GB, respectively.

ECM Proteins. ECM protein content was investigated through the conventional Bradford assay.[18] Proteins appear as a minor ECM constituent because only 10 mg/g ECM was observed. The molecular size distribution was nevertheless studied by SDS−PAGE. Figure 7 shows a single band corresponding to a MW of ∼37 kDa. This MW matches well that of flagellin, the constituent of flagellae, because MWs ranging from 41 to 36.7 kDa have been reported.[39,40] It is likely that this low amount of flagellin in ECM comes from the breakdown of flagellae or is released during dedifferentiation.

EPS Hydration. As expected, EPS are the major constituents of *P. mirabilis* ECM. This implies that the global physical properties of the slime mainly depend on the mechanical

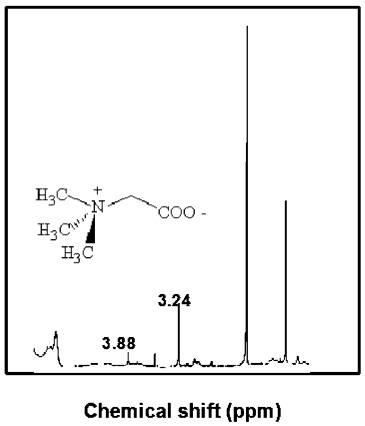

Figure 6. Partial ^{1}H NMR spectrum of the whole ECM in D_2O at 25 °C. The peaks at 3.88 and 3.24 ppm are characteristic of the GB methylene and methyl groups, respectively.

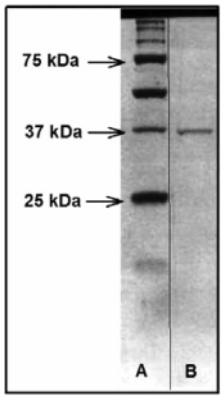

Figure 7. SDS−PAGE of ECM. Lane A, MW standards; lane B, ECM.

properties of the binary EPS mixture, which in turn must be ruled by the existence of a particular H bond network. Because it has been observed that the colony exhibits a low water activity, it was of interest to probe the EPS hydration process. Accordingly, water sorption/desorption was monitored through infrared spectroscopy. This vibrational spectroscopy is very useful in this context because it allows the simultaneous probing of water uptake, the evolution of the H bond network and the subsequent EPS conformational changes. Figure 8 displays the EPS FTIR-ATR spectra observed as a function of hydration. As mentioned in Experimental Section, sorption and desorption experiments have been performed repeatedly and have shown that the two processes are fully reversible. As expected, the high frequency domain (Figure 8A) mainly reflects water uptake through the increase of the large ν_{O-H} band ranging from 3600 to 2300 cm^{-1} as one goes from the anhydrous spectrum (lower 3000 cm^{-1} intensity) to the fully hydrated spectrum (larger 3000 cm^{-1} intensity). The lower frequency domain exhibits more interesting features (Figure 8B) because this domain contains the EPS spectral signature with very weak, if any, water contribution. Hence, spectral alterations in this domain are essentially linked to EPS conformational properties. One may focus on the 900−1200 cm^{-1} frequency range because it corresponds to sugar ring vibrations (900−1080 cm^{-1}) and to C−O−C inter ring bonds (1145 cm^{-1}). Spectral observations show that as hydration evolves continuously, spectral evolution exhibits marked discontinuities, which must correspond to the sudden conformational changes driven by solute−solvent reorganizations. Such a discontinuous evolution has yet been observed with hyaluronan.[22,23]

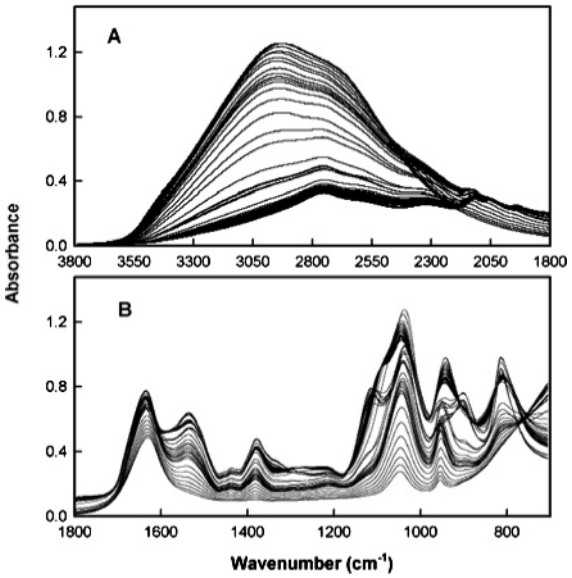

Figure 8. Hydration FTIR spectra of purified EPS. The Figure displays the EPS spectral evolution as a function of hydration. (A) High frequency domain; the hydration increases like the absorbance at 3000 cm^{-1}. (B) Low frequency domain. The lower, less structured spectrum is the more hydrated sample.

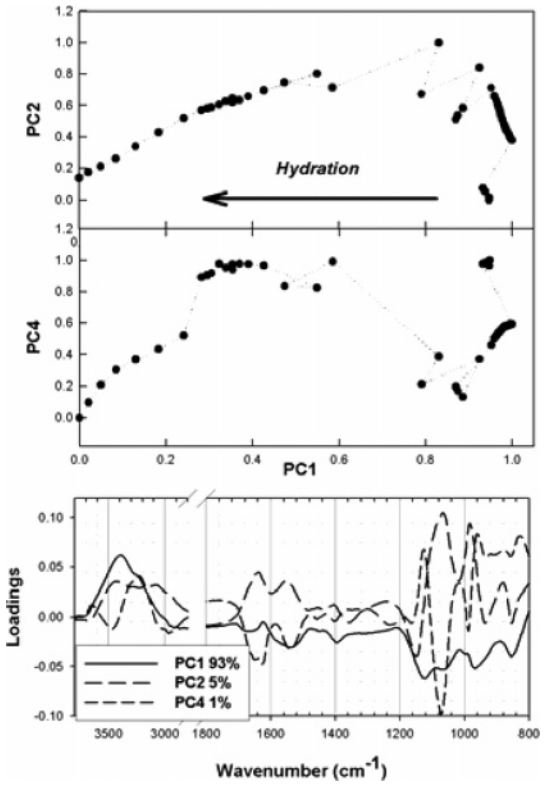

Figure 9. Principal component analysis of the EPS hydration spectra. The spectra displayed in Figure 8 were analyzed by PCA. The two upper panels feature the PCA map, PC1 mainly reflecting the extent of hydration. *X* loadings of PC1, PC2, and PC4 are displayed in the lower panel.

To get a clearer view of such bifurcations, a principal component analysis (PCA) was performed on the full spectral set. Figure 9 displays both PC maps (upper panel) along with the loadings corresponding to the most relevant principal components (lower panel). It is obvious that the first principal component, PC1 reflecting 93% of the total spectral variability, is related to the water uptake as deduced from large positive loadings in the ν_{O-H} frequency domain and negative loadings

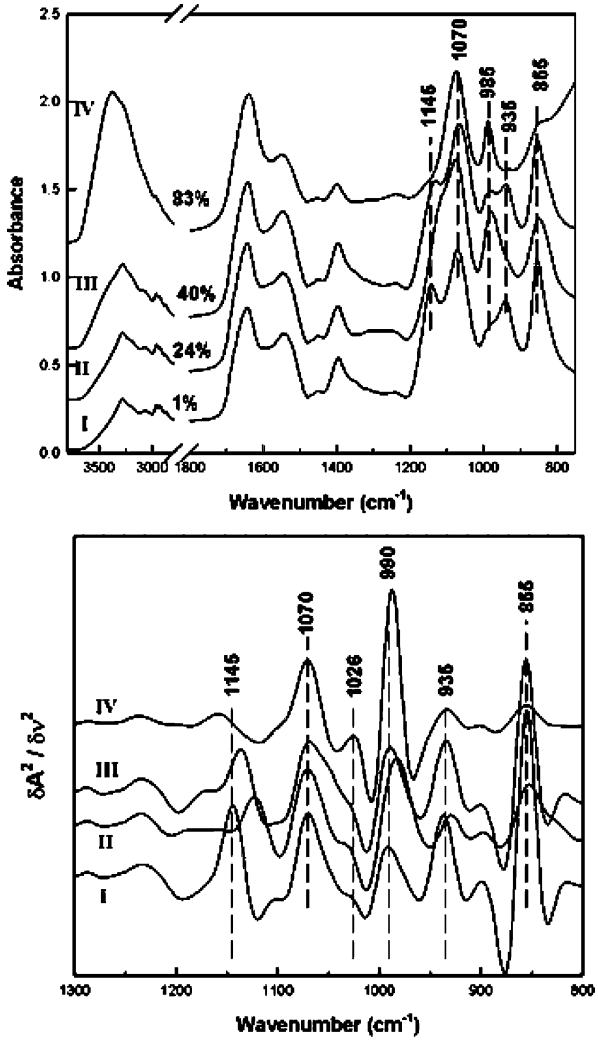

Figure 10. Classes of hydration EPS spectra. PCA helped in resolving EPS elementary spectra along the hydration axis. The four classes may be illustrated by typical spectra corresponding to the average of each cluster. Hence, spectra observed at 1, 24, 40, and 83% RH are representative of the four classes (upper panel). Also displayed is the spectra second derivative in a domain where EPS show up because water does not directly contribute to the absorbency in this frequency range (lower panel).

in the frequency range, where EPS contribution shows up. In contrast, both PC2 (5% of variability) and PC4 (1% of variability) exhibit large loadings in the 900−1200 cm^{-1} frequency domain. If one likens the PC1 score to the hydration extent, one can easily visualize (PCA maps) the aforementioned sharp discontinuities in the hydration process. They are featured by large complex distances (a PCA map is multidimensional) between spectral clusters. This analysis has allowed us to identify four elementary spectra related to four classes, I to IV, which roughly correspond to RH values of 1%, 24%, 40%, and 83%, respectively. These elementary spectra along with their second derivative are displayed in Figure 10. The main spectral evolution concerns: (i) the progressive decrease of the 855 cm^{-1} band; (ii) a nonlinear evolution of the 935/985 cm^{-1} doublet; the 935 cm^{-1} mode completely vanishing in the classes II and IV; (iii) the progressive increase of a H bonded ν_{C-OH} group; and (iv) the vanishing and low-frequency shift of the 1145 cm^{-1} as water uptake progresses. Altogether, these findings reveal marked alterations of the EPS conformations in relation to perturbations of the H bond lattice mainly involving the ν_{C-OH} bands of alcohols.

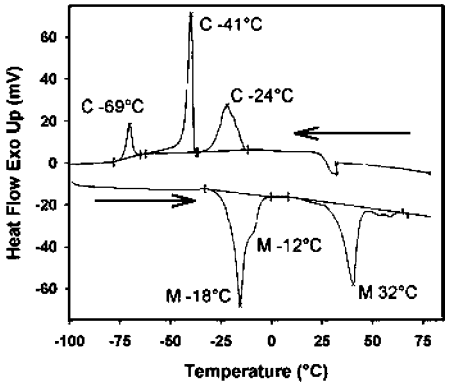

Figure 11. DSC thermogram of purified EPS. The Figure displays a typical thermogram observed at 300 g/L. The arrows indicate the thermal ramp direction. M, melting; C, crystallization.

Temperature Driven Phase Transitions. To further characterize the functional properties of the ECM exopolysaccharides, differential scanning calorimetry has been performed with the purified EPS fraction. Crystallization and melting transitions have been looked for in the −100 to +80 °C thermal range. Repetitive up and down thermal ramps have been performed in order to progressively vary the EPS concentration. Indeed, each heating up to 80 °C led to progressive water loss, which allowed for the variation of the EPS concentration from 100 to 550 g/L. Figure 11 displays the thermogram observed at the physiologic concentration, that is, 300 g/L. First, one can note sharp peaks at −41 °C (crystallization) and −18 °C (melting), which likely reflect the bound water phase transition. Because of the high EPS concentration, most of the water present in the sample interacts with the polysaccharide molecules (the so-called bound water), which results in a drastic thermal shift of these transitions. Besides, other crystallization and melting transitions are observed, which are characterized by wider peaks. Such a widening of the enthalpic transitions may be due to partial crystallization/melting transitions as observed in heterogeneous systems, especially in semicrystalline media. It is of interest that a melting transition occurs at 32 °C, which is close to that at which the colony grows. This strongly suggests that part of the slime could be crystallized, that is, the ECM would exhibit the characteristics of a semicrystalline medium.

EPS Mechanical Properties. For EPS solutions at concentrations up to 100 g/L, only the Newtonian viscosity could be measured. It was shown to be of the order of magnitude of the viscosity of water, that is ∼1 mPa s. This result clearly shows that the low concentration EPS solutions mainly behave like simple fluids that are non-structured fluids. On the contrary, for EPS samples at concentrations ranging from 100 to 300 g/L, the solutions were shown to exhibit viscoelastic behaviors, as shown in Figure 12 for a 300 g/L EPS solution. The linear viscoelastic response is discussed in terms of the storage modulus, G', characterizing the elastic energy stored in the solution, and of the loss modulus, G'', characterizing the viscous dissipation within the sample. Figure 12A shows that the linear viscoelastic regime is limited to low strains, of a few %, which suggests that the structure responsible for the viscoelasticity is somewhat fragile. Moreover, it clearly shows that the linear rheological behavior is mainly elastic, $G' > G''$, which indicates that the structure of the concentrated EPS is more cohesive than dissipative. Figure 12B confirms this result: it shows that the viscoelastic moduli G' and G'' do not significantly depend on the frequency so that $G' > G''$ over the whole frequency range explored. In a complex fluid, a predominant elastic behavior is the signature of the existence of a network.[41] In the case of

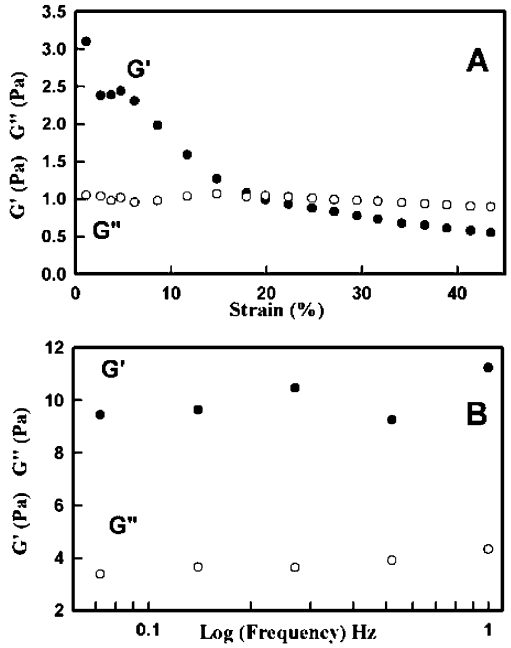

Figure 12. Viscoelastic behavior of a 300 g/L EPS solution. Viscoelastic moduli G' and G'' as a function of strain (A) and frequency (B).

macromolecular systems, the network is formed through either physical or chemical intermolecular interactions. Therefore, the rheological results presented in this study tend to show that, above an EPS concentration of ∼300 g/L, an intermolecular network forms. The connections of this network are most likely formed via physical, and not chemical, intermolecular interactions, which would explain the fragile character of the elastic structure. The numerous H bonds present in the system are certainly the best candidates for these physical intermolecular interactions. However, the rheological investigation does not allow for discriminating the two EPS populations analyzed by SEC.

Semicrystalline Properties of the ECM. The functional properties of the ECM, as deduced from rheology, infrared spectroscopy, and calorimetry, suggest that the *P. mirabilis* ECM exhibits semicrystalline properties. This drove us to look for the presence of crystal objects within the ECM. Accordingly, both purified EPS and lipid fractions have been observed in polarizing microscopy. In the case of EPS, diluted (about 60 g/L) solutions were allowed to age, and consequently to slowly concentrate, for days. This results in the formation of two kinds of crystalline objects. First, objects that look like sphérolites (Figure 13A and C), as observed between crossed polarizers and in phase contrast microscopy, exhibiting diameters of about 100 μm. The spherolite's typical Malt cross was observed in such samples (Figure 13C). Second, spiked crystals were observed with spikes reaching up to 1 μm. Similarly, ECM lipid extracts were analyzed. Figure 13D displays a crystal object whose pattern also recalls the spherolitic organization. As a whole, the presence of spherolites formed either from EPS or PGL further supports the hypothesis that *P. mirabilis* ECM behaves as a semicrystalline continuum.

The present study aims at characterizing the biochemical and functional properties of a *P. mirabilis* colony. In this article, we have focused on the extracellular matrix, the slime, which is known to be determinant in any colony behavior. If the massive production of exopolysaccharides and/or biosurfactants is well documented, a possible role in the dynamics of the bacterial multicellar entity has been somehow disregarded if

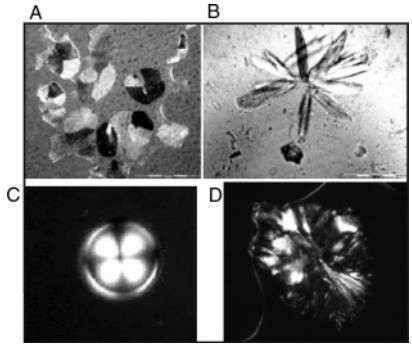

Figure 13. Spherolites and crystalline objects observed in the EPS and lipid ECM fractions. (A, B, and C) EPS observed under crossed polarizers. (D) PGL observed under similar conditions.

one except the hydrodynamic approach of bacterial colonies, which emphasize the relationships between colony patterns and diffusion processes.[42] Especially in the case of the *P. mirabilis* enigma, very little attention has been paid to the ECM molecular composition and the mechanical properties that follow. On the one hand, the present data show that this composition is much more complex than expected because a binary EPS mixture has been identified along with the presence of a novel phenoglycolipid and glycinebetaine, an effective osmoprotectant. On the other hand, the ECM exhibits viscoelastic properties and phase transitions that strongly suggest that it behaves as a semicristalline continuum. Such media are characterized by auto-organization phenomena between biomolecules that confer unique mechanical properties. It is, therefore, interesting to better understand how these features are of consequence in the colony's dynamics.

P. mirabilis produces, before any swarming phase, a binary mixture of EPS with very distinct molecular weights. It is unusual that low MW EPS are present in bacterial colonies. In the present case, it is also noteworthy that the relative proportions of the high (300 kDa) and low (1 kDa) compounds depend on growing conditions, namely, planctonic or sessile conditions. Moreover, in the case of sessile conditions, the bacterium also responds to variations in the agar support hydration. This matches well the observed dependence between colony patterns and agar concentration.[43] In contrast to the general observation that a particular bacterium produces a particular exopolysaccharide, *P. mirabilis* is able to cope with distinct environmental conditions by modulating the EPS biosyntheses. This makes sense if one recalls how the planctonic and sessile modes interfere with nutrient uptake. In one case, filamentous polysaccharides help in trapping solutes in the liquid culture, and in the other case, nutrients must be pumped up from the agar support. The latter process implies that osmotic forces must drive net water and solutes fluxes from the agar to the colony. Because osmotic pressure is proportional to the number of molecules and not their size, cell economy likely favors the production of numerous small molecules (1 kDa) rather than large ones (300 kDa). The concomitant presence of GB in the ECM reinforces this hypothesis. Indeed, GB is actively synthesized or accumulated by bacteria in the case of an osmotic shock.[38] This concomitance has yet been reported in the case of *E. coli* K-12 biofilm,[44] where GB was observed to enhance the colanic acid synthesis. More generally, it has been assessed that an osmotic shock is responsible for large transcriptional changes because up to 38% of the genes are altered in their expression.[45] Hence, this may link particular EPS syntheses with the extent of the osmotic stress, which finally depends on agar concentration. Altogether, the predominance of a small MW EPS compound and GB in the slime suggests that *P. mirabilis* faces drastic osmotic conditions, which must be the *sine qua non* conditions to attract water and nutrients from the agar support.

Besides EPS, a novel PGL compound has been identified in the *P. mirabilis* ECM by different complementary techniques. So far, such a glycolipid has only been detected in the *Mycobacterium* genus for which it confers antigenicity.[32] Rhamnoplids, another kind of glycolipid, are more often encountered, for example in *Pseudomonas* biofilms.[30] Different spectral analyses clearly show that the PGL identified in *P. mirabilis* slime is distinct from typical rhamnolipids because the latter does not contain a phenol group. Such surfactants are known to reduce friction between the bacteria and the support. It has also been reported that their potential in bioremediation originates in micelle formation above a critical concentration;[46] this certainly is relevant, regarding the mechanical properties of the slime. In the case of *P. mirabilis* ECM, the role of PGL remains unascertained. Besides this potential contribution to the slime viscoelasticity, it may be hypothesized that this compound may contribute to *P. mirabilis* virulence because it has been shown in a particular experimental model that PGL biosynthesis was associated with a hypervirulent phenotype.[47]

Once the prominent biomolecules have been identified in the ECM, it was critical to investigate their behavior within the slime. Swarming is a particular mode of cell motility, which relies on fast motions linking bacteria in rafts following a single trajectory. Such fast motions (60 μm/s) have to necessarily cope with the continuum viscosity, which in turn must be altered because of the shear stress imposed by the motion of bacterial rafts. The phase transitions observed in purified EPS fractions clearly show that, at their physiological concentration ($\approx$300 g/L), EPS compounds are structured in large networks, very likely due to extensive intermolecular H bondings. The progressive hydration study of EPS reveals the occurrence of discontinuities, which must originate in large conformational changes driven by the alteration of the solute−solvent interactions. Similarly, DSC experiments reveal melting and crystallization transitions, which are characteristic of semicristalline media. In addition, the presence of a melting transition very close (32 °C) to the physiological temperature at which bacteria are grown (37 °C) reinforces the hypothesis that auto-organization phenomena occur in the *P. mirabilis* ECM. Polarization microscopy brings additional evidence that both EPS and PGL may auto-organize because spherolitic objects, currently observed in semicrystalline media, were detected. Such behavior is usually observed when large polymers interact.[48,49] In the present case, EPS are essentially low MW compounds with a very minor fraction of a large MW compound. Nevertheless, rheology unambiguously indicates that the EPS binary mixture exhibits a high elastic modulus behavior, which vanishes at subphysiological concentrations. Such a behavior has yet been described on various biofilms by creep test.[50] Viscoelasticity implies that the low MW compound (1 kDa) interacts within a complex H bond network, which confers the observed mechanical properties to the slime. However, the interactions between the 1 and 300 kDa compounds remain unrevealed. One may hypothesize that the larger compound may acts as a plasticizer for the small compounds, whose intrinsic properties likely lead to crystallization. It is also tempting to associate the unusual occurrence of a small MW EPS compound with the tuning of the ECM viscoelastic behavior in such a way that fast bioconvection motions may occur. Indeed, such fast motions are unique and must rely on defined, particular, mechanical properties. The modulation of EPS biosyntheses in response to distinct envi-

ronmental conditions suggests that *P. mirabilis* designs the molecular structure of the exoproducts in order to achieve the particular functional properties essential for active swarming. If this is assessed, this means that swarming ability and ECM molecular networks are strongly correlated. The purpose of this work is to get better insights of the role played by ECM in the control of swarming migration. If exoproducts such as biosurfactants have been found to be essential for cell motility in strains such as *Serratia liquefaciens*,[51,52] a potential role in the regulation of this process has never been clearly demonstrated. That *S. liquefaciens* swarming is controlled by AHL autoinducers is noteworthy. The lack of such exocellular mediators in the *P. mirabilis* strain suggests that a distinct mechanism rules the periodicity and synchronicity of the swarming process.

In conclusion, one may assess the viscoelastic behavior of the ECM, which is mainly due to the existence of large molecular networks whose properties highly depend on their concentration and hence on their hydration. As a consequence, the question of the water activity within the colony is addressed because swarming depends on the mechanical properties of the slime. In the article following this one, we have analyzed the rheological properties of the whole intact colony and investigated the water balance variations during the alternation of the swarming and consolidation phases.

Abbreviations

AHL: acyl homoserine lactone
CPS: capsular polysaccharide
DSC: differential scanning calorimetry
ECM: extracellularr matrix
EPS: exopolysaccharides
FTIR: Fourier transform infrared
GB: glycinebetaine
HMBC: heteronuclear multiple bond coherence
HMQC: heteronuclear multiple quantum coherence
HPAEC: high performance anion exchange chromatography
LB: Luria Bertani
LPS: lipopolysaccharide
NMR: nuclear magnetic resonance
PGL: phenoglycolipid
SDS−PAGE: sodium dodecyl sulfate polyacrylamide gel electrophoresis
SEC: size exclusion chromatography
TLC: thin layer chromatography

References and Notes

(1) Shapiro, J. A. Multicellularity: The Rule, Not the Exception. In *Bacteria as Multicellular Organisms*; Shapiro, J. A., Dworkin, M., Eds.; Oxford University Press: New York, 1997; pp 14−49.
(2) Costerton, J. W.; Lewandowski, Z.; Caldwell, D. E.; Korber, D. R.; Lappin-Scott, H. M. Microbial biofilms. *Annu. Rev. Microbiol.* **1995**, *49*, 711−745.
(3) Eberl, L.; Christiansen, G.; Molin, S.; Givskov, M. Differentiation of *Serratia liquefaciens* into swarm cells is controlled by the expression of the flhD master operon. *J. Bacteriol.* **1996**, *178*, 554−559.
(4) Bassler, B. L.; Wright, M.; Silverman, M. R. Multiple signalling systems controlling expression of luminescence in *Vibrio harveyi*: sequence and function of genes encoding a second sensory pathway. *Mol. Microbiol.* **1994**, *13*, 273−286.
(5) Allison, C.; Hughes, C. Bacterial swarming: an example of prokaryotic differentiation and multicellular behaviour. *Sci. Prog.* **1991**, *75*, 403−422.
(6) Fraser, M. F.; Hughes, C. Swarming motility. *Curr. Opin. Microbiol.* **1999**, *2*, 630−635.
(7) Rauprich, O.; Matsushita, M.; Weijer, C. J.; Siegert, F.; Esipov, S. E.; Shapiro, J. A. Periodic phenomena in *Proteus mirabilis* swarm colony development. *J. Bacteriol.* **1996**, *178*, 6525−6538.
(8) Shapiro, J. A. The significances of bacterial colony patterns. *Bioessays.* **1995**, *17*, 597−607.
(9) Schneider, R.; Lockatell, C. V.; Johnson, D.; Belas, R. Detection and mutation of luxS-encoded autoinducer in *Proteus mirabilis*. *Microbiology* **2002**, *148*, 773−782.
(10) Belas, R.; Schneider, R.; Melch, M. Characterization of *Proteus mirabilis* precocious swarming mutants: Identification of *rsbA* encoding a regulator of swarming behavior. *J. Bacteriol.* **1998**, *180*, 6126−6139.
(11) Sturgill, G.; Rather, P. N. Evidence that putrescine acts as an extracellular signal required for swarming in *Proteus mirabilis*. *Mol. Microbiol.* **2004**, *51*, 437−446.
(12) Allison, C.; Lai, H.-C.; Gygi, D.; Hughes, C. Cell differentiation of *Proteus mirabilis* is initiated by glutamine, a specific chemoattractant for swarming cells. *Mol. Microbiol.* **1993**, *8*, 53−60.
(13) Gué, M.; Dupont, V.; Dufour, A.; Sire, O. Bacterial swarming: a biochemical time-resolved FTIR-ATR study of *Proteus mirabilis* swarm-cell differentiation. *Biochemistry* **2001**, *40*, 11938−11945.
(14) Keirsse, J.; Lahaye, E.; Bouter, A.; Dupont, V.; Boussard-Plédel, C.; Bureau, B.; Adam, J. L.; Monbet, V.; Sire, O. Mapping bacterial surface population physiology in real-time: infrared spectroscopy of *Proteus mirabilis* swarm colonies. *Appl. Spectrosc.* **2006**, *60*, 584−591.
(15) Matsuyama, T.; Takagi, Y.; Nakagawa, Y.; Itoh, H.; Wakita, J.; Matsushita, M. Dynamic aspects of the structured cell population in a swarming colony of *Proteus mirabilis*. *J. Bacteriol.* **2000**, *182*, 385−393.
(16) Claret, L.; Hughes, C. Rapid turnover of FlhD and FlhC, the flagellar regulon transcriptional activator proteins, during *Proteus* swarming. *J. Bacteriol.* **2000**, *182*, 833−836.
(17) Porter, K. G.; Feig, Y. S. The use of DAPI for identifying and counting aquatic microflora. *Limnol. Oceanogr.* **1980**, *25*, 943−948.
(18) Bradford, M. M. A rapid and sensitive for the quantitation of microgram quantities of protein utilizing the principle of protein-dye binding. *Anal. Biochem.* **1976**, *72*, 248−254.
(19) Laemmli, U. K. Cleavage of structural proteins during the assembly of the head of bacteriophage T4. *Nature* **1970**, *227*, 680−685.
(20) Bligh, E. G.; Dyer, W. J. A rapid method of total lipid extraction and purification. *Can. J. Biochem. Physiol.* **1959**, *37*, 911−917.
(21) Venkata Ramana, K.; Karanth, N. G. Factors affecting biosurfactant production using *Pseudomonas aeruginosa* CFTR-6 under submerged conditions. *J. Chem. Technol. Biotechnol.* **1989**, *45*, 249−257.
(22) Haxaire, K.; Marechal, Y.; Milas, M.; Rinaudo, M. Hydration of hyaluronan polysaccharide observed by IR spectrometry. II. Definition and quantitative analysis of elementary hydration spectra and water uptake. *Biopolymers* **2003**, *72*, 149−161.
(23) Haxaire, K.; Marechal, Y.; Milas, M.; Rinaudo, M. Hydration of polysaccharide hyaluronan observed by IR spectrometry. I. Preliminary experiments and band assignments. *Biopolymers* **2003**, *72*, 10−20.
(24) Beynon, L. M.; Dumanski, A. J.; McLean, R. J.; MacLean, L. L.; Richards, J. C.; Perry, M. B. Capsule structure of *Proteus mirabilis* (ATCC 49565). *J. Bacteriol.* **1992**, *174*, 2172−2177.
(25) Gygi, D.; Rahman, M. M.; Lai, H. C.; Carlson, R.; Guard-Petter, J.; Hughes, C. A cell-surface polysaccharide that facilitates rapid population migration by differentiated swarm cells of *Proteus mirabilis*. *Mol. Microbiol.* **1995**, *17*, 1167−1175.
(26) Rahman, M. M.; Guard-Petter, J.; Asokan, K.; Hughes, C.; Carlson, R. W. The structure of the colony migration factor from pathogenic *Proteus mirabilis*. A capsular polysaccharide that facilitates swarming. *J. Biol. Chem.* **1999**, *274*, 22993−22998.
(27) Sutherland, I. W. Biosynthesis and composition of gram-negative bacterial extracellular and wall polysaccharides. *Annu. Rev. Microbiol.* **1985**, *39*, 243−270.
(28) Gunther, N. W. T.; Nunez, A.; Fett, W.; Solaiman, D. K. Production of rhamnolipids by *Pseudomonas chlororaphis*, a nonpathogenic bacterium. *Appl. Environ. Microbiol.* **2005**, *71*, 2288−2293.
(29) Siegmund, I.; Wagner, F. New method for detecting rhamnolipids excreted by *Pseudomonas* species during growth on mineral agar. *Biotechnol. Tech.* **1991**, *5*, 265−268.
(30) Sim, L.; Ward, O. P.; Li, Z. Y. Production and characterization of a biosurfactant isolated from *Pseudomonas aeruginosa* UW-1. *J. Ind. Microbiol. Biotechnol.* **1997**, *19*, 232−238.

(31) Deziel, E.; Lepine, F.; Milot, S.; Villemur, R. Mass spectrometry monitoring of rhamnolipids from a growing culture of *Pseudomonas aeruginosa* strain 57RP. *Biochim. Biophys. Acta* **2000**, *1485*, 145−152.
(32) Hunter, S. W.; Brennan, P. J. A novel phenolic glycolipid from *Mycobacterium leprae* possibly involved in immunogenicity and pathogenicity. *J. Bacteriol.* **1981**, *147*, 728−735.
(33) Hunter, S. W.; Brennan, P. J. Further specific extracellular phenolic glycolipid antigens and a related diacylphthiocerol from *Mycobacterium leprae*. *J. Biol. Chem.* **1983**, *258*, 7556−7562.
(34) Camphausen, R. T.; Jones, R. L.; Brennan, P. J. A glycolipid antigen specific to *Mycobacterium paratuberculosis*: structure and antigenicity. *PNAS U.S.A.* **1985**, *82*, 3068−3072.
(35) Perez, E.; Constant, P.; Lemassu, A.; Laval, F.; Daffe, M.; Guilhot, C. Characterization of three glycosyltransferases involved in the biosynthesis of the phenolic glycolipid antigens from the *Mycobacterium tuberculosis* complex. *J. Biol. Chem*. **2004**, *279*, 42574−42578.3.
(36) Fujiwara, T.; Hunter, S. W.; Cho, S. N.; Aspinall, G. O.; Brennan, P. J. Chemical synthesis and serology of disaccharides and trisaccharides of phenolic glycolipid antigens from the leprosy bacillus and preparation of a disaccharide protein conjugate for serodiagnosis of leprosy. *Infect. Immun.* **1984**, *43*, 245−252.
(37) Vercellone, A.; Puzo, G. New-found phenolic glycolipids in *Mycobacterium bovis* BCG. Presence of a diglycosylated glycolipid. *J. Biol. Chem.* **1989**, *264*, 7447−7454.
(38) Csonka, L. N. Physiological and genetic responses of bacteria to osmotic stress. *Microbiol. Rev.* **1989**, *53*, 121−147.
(39) Bahrani, F. K.; Johnson, D. E.; Robbins, D.; Mobley, H. L. *Proteus mirabilis* flagella and MR/P fimbriae: isolation, purification, N-terminal analysis, and serum antibody response following experimental urinary tract infection. *Infect. Immun.* **1991**, *59*, 3574−3580.
(40) Belas, R.; Erskine, D.; Flaherty, D. *Proteus mirabilis* mutants defective in swarmer cell differentiation and multicellular behavior. *J. Bacteriol.* **1991**, *173*, 6279−6288.
(41) Larson, R. G. In *The Structure and Rheology of Complex Fluids*; Oxford University Press: New York, 1999.
(42) Mimura, M.; Sakaguchi, H.; Matsushita, M. Reaction-diffusion modeling of bacterial colony patterns. *Physica A* **2000**, *282*, 283−303.
(43) Harshey, R. M. Bacterial motility on a surface: many ways to a common goal. *Annu. Rev. Microbiol.* **2003**, *57*, 249−273.
(44) Sledjeski, D. D.; Gottesman, S. Osmotic shock induction of capsule synthesis in *Escherichia coli* K-12. *J. Bacteriol.* **1996**, *178*, 1204−1206.
(45) Prigent-Combaret, C.; Vidal, O.; Dorel, C.; Lejeune, P. Abiotic surface sensing and biofilm-dependent regulation of gene expression in *Escherichia coli*. *J. Bacteriol.* **1999**, *180*, 5993−6002.
(46) Helvacci, S. S.; Peker, S.; Özdemir, G. Effect of electrolytes on the surface behaviour of rhamnolipides R1 and R2. *Colloid Surf., B* **2004**, *35*, 225−233.
(47) Reed, M. B.; Domenech, P.; Manca, C.; Su, H.; Barczak, A. K.; Kreiswirth, B. N.; Kaplan, G.; Barry, C. E., III. A glycolipids of hypervirulent tuberculosis strains that inhibits the innate immune response. *Nature* **2004**, *431*, 84−87.
(48) Giraud-Guillé, M. M.; Besseau, L.; Martin, R. Liquid crystalline assemblies of collagen in bone and in vitro systems. *J. Biomech. Eng.* **2003**, *36*, 1571−1579.
(49) Giraud-Guillé, M. M. Liquid crystalline order of biopolymers in cuticles and bones. *Microsc. Res. Tech.* **1994**, *27*, 420−428.
(50) Shaw, T.; Winston, M.; Rupp, C. J.; Klapper, I.; Stoodley, P. Commonality of elastic relaxation times in biofilms. *Phys. Rev. Lett.* **2004**, *93*, 098102-1−098102-4.
(51) Lindum, P. W.; Anthoni, U.; Christophersen, C.; Eberl, L.; Molin, S.; Givskov, M. *N*-acyl-L-Homoserine lactone autoinducers control production of an extracellular lipopeptide biosurfactant required for swarming motility of *Serratia liquefaciens* MG1. *J. Bacteriol.* **1998**, *180*, 6384−6388.
(52) Eberl, L.; Molin, S.; Givskov, M. Surface motility of *Serratia liquefaciens* MG1. *J. Bacteriol.* **1999**, *181*, 1703−1712.

BM061181L